EDITORIAL

Is Patlak *y*-intercept a relevant metrics?

Eric Laffon [1,2,3,4] · Roger Marthan [1,2,3]

In daily positron emission tomography (PET) imaging, whole-body (WB) static acquisitions allow the nuclear physicians to quantitatively report on the tracer uptake in tissues by using the standardized uptake value (SUV), which is the tissue activity concentration normalized to the injected dose divided by patient's weight [1]. However, this semi-quantitative uptake index has limitations, e.g., SUV in [^{18}F]-fluoro-deoxy-glucose (FDG) PET imaging is only a surrogate for assessing the increased glycolysis of cancer cells. Kinetic model analyses have been implemented to more specifically assess tracer uptake, of which Patlak graphical analysis (PGA) is considered a gold standard, assuming irreversible trapping of the tracer [2–4]. PGA requires dynamic acquisition, knowledge of the blood time-activity curve (i.e., the so-called input function (IF)), and steady state of the system. It then provides an estimate of the tracer uptake-rate constant (i.e., the net influx constant: K_i) in the tissue of interest, which is the slope of a linear fit. However, this linear fit also provides a *y*-intercept (i.e., Y_0) that, potentially, might be considered as a metrics, independent of K_i, to further characterize the tissue of interest [5, 6].

Performing PGA at the voxel level can provide PGA-based WB parametric images in routine practice whose clinical interest may be decisive for the patient care,

especially since dynamic WB PET imaging and 194-cm-long PET/CT scanners are now available [6, 7]. However, whereas K_i-parametric imaging has been extensively investigated, the potential ability of PGA to complementarily provide Y_0-parametric imaging remains to be clarified. Therefore, the current theoretical study aims at investigating whether Y_0 may actually be a relevant metrics. For this, its different contributions have been identified along with their relative magnitude and their sources of variability in FDG PET imaging.

Theory

A two-tissue compartment model is considered involving trapped-tracer and free-tracer compartments, where the rate constants K_1 and k_2 account for forward and reverse transport between blood and reversible compartment, and k_3 and k_4 account for forward and reversed transport between reversible and trapping compartment, respectively (Fig. 1). PGA assumes irreversible trapping of the tracer, that is, k_4 is considered negligible. The activity at time t per tissue volume unit (in kBq mL^{-1}) from free and trapping compartment, without correction for physical decay, is the convolution product (denoted by $\otimes$) of the impulse response function of the system with the IF, i.e., with $C_p(t)$ [4]:

$$C_{F+T}(t) = \left\{ [K_1 k_2/(k_2 + k_3)] \times e^{-(k2+k3+\lambda)\times t} + K_i \times e^{-\lambda \times t} \right\} \otimes C_p(t) \quad (1)$$

where $K_i = k_1 k_3/(k_2 + k_3)$ (in mL min^{-1} mL^{-1}) and λ is the tracer decay-rate constant (in min^{-1}). The total tissue activity at time t per tissue volume unit (i.e., $C_{Tot}(t)$; in kBq mL^{-1}; uncorrected for physical decay) additionally involves the blood-volume fraction (V_b; in mL mL^{-1}). For a tri-exponentially decaying IF (uncorrected for physical decay), i.e., $C_p(t) = \Sigma A_i \times e^{-bi \times t}$ (b_i in min^{-1} and A_i in kBq mL^{-1}), it writes

---

This article is part of the Topical Collection on Editorial

✉ Eric Laffon
elaffon@u-bordeaux.fr

1 CHU de Bordeaux, 33000 Bordeaux, France

2 Centre de Recherche Cardio-Thoracique de Bordeaux, University of Bordeaux, 33000 Bordeaux, France

3 Centre de Recherche Cardio-Thoracique de Bordeaux, INSERM U-1045, 33000 Bordeaux, France

4 Service de Médecine Nucléaire, Hôpital du Haut-Lévèque, Avenue de Magellan, 33604 Pessac, France
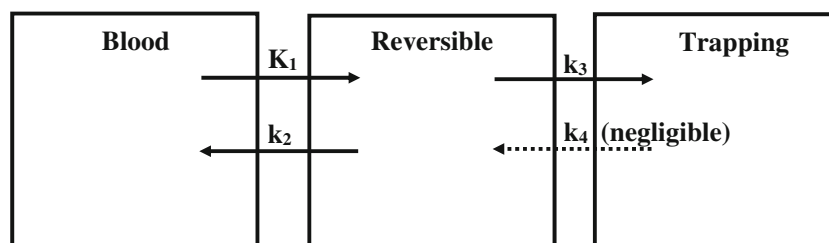
Fig. 1 The two-tissue compartment model involves blood, intermediate reversible compartment and trapping compartment, which are connected with transport-rate constants. In the PGA framework, the rate constant k_4

accounting for reversed transport between trapping and reversible compartment is considered negligible

$$C_{Tot}(t) = V_b \times \left(\Sigma A_i \times e^{-bi \times t}\right) + \Sigma A_i$$
$$\times \left[K_1 k_2/(k_2 + k_3)(k_2 + k_3 + \lambda - b_i)\right]$$
$$\times \left[e^{-bi \times t} - e^{-(k2+k3+\lambda) \times t}\right] + (1 - V_b) \times K_i$$
$$\times \left\{\Sigma A_i \times \left[1/(\lambda - b_i)\right] \times \left[e^{-bi \times t} - e^{-\lambda \times t}\right]\right\} \quad (2)$$

where taking into account blood-volume fraction also leads to correcting K_i to $(1 - V_b) \times K_i$.

PGA consists of dividing each side of Eq. 2 by $C_p(t)$, yielding

$$C_{Tot}(t)/C_p(t) = V_b + \Sigma V_i + (1 - V_b) \times K_i \times t_s \quad (3)$$

where V_i (in mL mL^{-1}) represents:

$$V_i = \left\{A_i \times \left[K_1 k_2/(k_2 + k_3)(k_2 + k_3 + \lambda - b_i)\right]\right. \quad (4)$$
$$\left. \times \left[e^{-bi \times t} - e^{-(k2+k3+\lambda) \times t}\right]\right\}/\left(\Sigma A_i \times e^{-bi \times t}\right)$$

and "t_s" is the so-called stretched time, which is given by

$$t_s = \left\{\Sigma A_i \times \left[1/(\lambda - b_i)\right] \times \left[e^{-bi \times t} - e^{-\lambda \times t}\right]\right\}/\left(\Sigma A_i \times e^{-bi \times t}\right) \quad (5)$$

For the period $t \geq t^*$ after tracer injection, that is, when reversible compartments are in effective steady state with blood plasma, it is assumed that the two first (rapid) IF exponential functions have decayed to zero, i.e., b_1 and $b_2 >> b_3$, thus simplifying Eq. 4 to

$$V_i = \left\{A_i \times \left[K_1 k_2/(k_2 + k_3)(k_2 + k_3 + \lambda - b_i)\right]\right. \quad (6)$$
$$\left. \times \left[e^{-bi \times t} - e^{-(k2+k3+\lambda) \times t}\right]\right\}/\left[A_3 \times e^{-b3 \times t}\right]$$

Results

Figure 2 illustrates PGA that displays the ratio $C_{Tot}(t)/C_p(t)$ versus the stretched time t_s. For the period $t \geq t^*$, and, hence, $t_s \geq t_s^*$, the steady-state uptake-rate constant K_i of the tissue of interest (more precisely, $(1 - V_b) \times K_i$) can be estimated as the slope of a linear fit whose intercept is $Y_0 = V_b + \Sigma V_i = V_b + V_1 + V_2 + V_3$.

Numerical estimates of V_1, V_2, V_3, and V_b were calculated from published literature data for (decay-corrected) ^{18}F-FDG IF [8] and applied to a typical lung tumor [6]: $b_1 - \lambda = 9.33$, $b_2 - \lambda = 0.289$, $b_3 - \lambda = 0.013$, $K_1 = 0.301$, $k_2 = 0.864$, $k_3 = 0.047$ min^{-1}, and $V_b = 0.066$ mL mL^{-1}. From Eq. 6, since $(k_2 + k_3) >> (b_3 - \lambda)$, i.e., $0.911 >> 0.007$, then V_3 is $K_1 k_2/[(k_2 + k_3)(k_2 + k_3 + \lambda - b_3)] = 0.317$ mL mL^{-1}, i.e., a figure about $+2\%$ greater than the so-called initial distribution volume $V_0 = K_1 k_2/(k_2 + k_3)^2 = 0.313$ mL mL^{-1} obtained when IF is held constant (i.e., $b_3 - \lambda = 0$) [4]. Furthermore, when $t > 5 \times Ln2/(b_2 - b_3) = 13$ min (i.e., t greater than a full decay time of the exponential function involving $b_2 - b_3$), the contribution V_2, and, a fortiori, the contribution V_1, have decayed to zero. As a result, in the present lung tumor example, the y-intercept is expected to be $Y_0 = V_b + V_3 = 0.383$ mL mL^{-1}, i.e., a figure about $+22\%$ greater than V_0. Noteworthy, as a benchmark, a (decay-corrected) rate constant of 0.043 min^{-1}, corresponding to a full decay time of $5 \times Ln2/0.043 = 81$ min postinjection, leads to a V_3 value that is $+5\%$ greater than V_0.
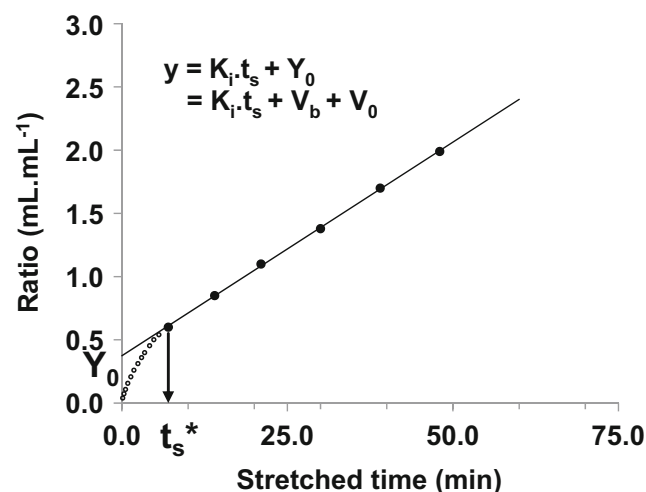

Fig. 2 Illustration of PGA (the tracer is not specified). After t_s^*, data points are used for PGA linear fit (full circles). Before t_s^*, data points are not involved in the fit (empty circles). The steady-state uptake-rate constant is the linear fit slope: $K_i = 0.0338$ mL min^{-1} mL^{-1}. The current study aims at identifying the different contributions involved in the linear fit y-intercept, whose value is, here, $Y_0 = 0.3740$ mL mL^{-1}

Discussion

The interpretation of Patlak y-intercept requires identifying its different contributions along with their relative magnitude and their sources of variability. Theory and numerical estimation have shown that $Y_0 = V_b + V_3$. First, the blood-volume fraction V_b depends on the tissue of interest. In the lung tumor example investigated with FDG, V_b represents 17% of Y_0 whereas, in some liver tumors, V_b may represent up to 54% of an average Y_0-value of 0.53 mL mL^{-1} [9], thus stressing that Y_0 actually involves V_b and V_3 in unknown proportions. Second, it is usually reported in literature that $Y_0 = V_b + V_0 = V_b + K_1 k_2/(k_2 + k_3)^2$ from the situation where IF is held constant [4], whereas our derivation shows that $Y_0 = V_b + V_3$ from a real situation involving a tri-exponentially decaying IF. In other words, the former equality is an approximate that neglects the role in Y_0 of an actually time-decaying IF (more specifically, it neglects the term "$b_3 - \lambda$"; Eq. 6). The lung tumor example investigated with FDG shows a small relative difference of + 2% between V_3 and V_0, and the magnitude of this difference is, very likely, also small for tracers used in current practice, thus reasonably justifying the approximation $Y_0 \approx V_b + V_0$. Nevertheless, we suggest that the issue of a non-negligible relative difference (i.e., > 5%) between V_3 and V_0 should be further investigated in tissues showing various K_1, k_2, and k_3 values and for fast-clearance tracers. These tracers should have a decay-corrected rate constant of late-phase IF (i.e., $b_3 - \lambda$) greater than 0.043 min^{-1}, or equivalently, a decay-corrected IF reaching zero before 81 min post-injection. Furthermore, regarding the meaning of V_3 and V_0, whereas the former seems challenging, the latter (i.e., the meaning of $[K_1/(k_2 + k_3)] \times [k_2/(k_2 + k_3)]$) is the quantity defined by the steady-state distribution volume of the reversible compartment multiplied by the probability for a tracer molecule located in the reversible compartment to go back to blood. However, for all the above-addressed reasons, we suggest that the relevance of Y_0, which sums V_b and either V_3 or V_0 as an approximate, in unknown proportions, cannot be clearly identified.

Measurement uncertainty of V_b depends on the volume of interest (VOI) that encompasses the tissue of interest. This VOI may indeed include blood vessels whose diameter is greater than the greatest voxel size, which may participate or not in the tracer uptake by the tissue (i.e., the latter just carrying blood). As a consequence, at the voxel level, V_b may show a significant histological variability, ranging from a parenchyma feature, such as $V_b = 0.066$ mL mL^{-1} in the lung tumor example, to $V_b = 1$ for a voxel located inside a blood vessel, leading to $Y_0 = 1$ since $V_3 = 0$ and to a null value of the Patlak slope that estimates "$(1 - V_b) \times K_i$" (Eqs. 2 and 3). Thus, the outcome of an average V_b value over an arbitrary VOI, and, hence, the relative contribution of V_b in Y_0, may unpredictably increase with an irrelevant blood vessel amount. In such a

situation, we suggest that the histogram representing the percentage of all voxels included in the VOI for the range of the Y_0 values (that, to the very best of our knowledge, has not been made available by the manufacturers yet), might help in separating out an irrelevant blood vessel amount, since $V_b = 1$ for any voxel located inside a blood vessel. Furthermore, in FDG PET imaging, tumor heterogeneity metabolism may result in significantly different V_b values between regions showing high/low glucose-metabolism activity, thereby suggesting that the tumor-outlining method may be another origin of variability for V_b [10].

Since Y_0 is graphically assessed, the different graphical origins of its measurement uncertainty should also be addressed. First, in current practice, t^*, and hence, t_s^*, i.e., the stretched time of the linear fitting start, are not exactly known and, thereby, a too early start may lead to an underestimate of Y_0, as can be deducted from Fig. 2. More specifically, when $t < t^*$, V_2 involves an exponential function that has not decayed to zero yet (Eq. 6). In the lung tumor example investigated with ^{18}F-FDG, the time needed for this assumption to be valid can be estimated to be $5 \times \text{Ln2}/(b_2 - b_3) = 13$ min, to which must be added the time needed to reach steady state with blood plasma that is $5 \times \text{Ln2}/(k_2 + k_3) = 4$ min, leading then to $t^* = 17$ min. A variety of factors are involved in t^*, including bolus injection, cardiac output, renal functioning, tracer uptake by the whole tissues over the patient's body [11], and a priori unknown K_1, k_2, and k_3 values of the tissue of interest. Second, the linear fit slope estimate is provided with standard deviation, which may be large in voxel-wise parametric imaging [6]. As may be graphically deducted from Fig. 2, the greater the standard deviation of the slope, the greater the Y_0 measurement uncertainty. To illustrate, K_i reproducibility in malignant tumors has been estimated in a test-retest study to be about 18% (95% CI) [12]. Third, the possible occurrence of tracer-trapping reversibility, even of low amplitude (low k_4-value; Fig. 1), may generate an unpredictable slope-value underestimation, and, hence, an unpredictable Y_0 overestimation (thus associated to an unpredictable K_i underestimation) [13]. Finally, combining all the above-described origins of measurement uncertainty contributes to a substantial measurement uncertainty in the graphical assessment of Y_0.

Conclusion

Assuming irreversible trapping, PGA actually provides the steady-state uptake-rate constant of the tracer, more precisely "$(1 - V_b) \times K_i$", as the slope of a linear fit. The current theoretical study shows that the relevance of the linear fit y-intercept, i.e., Y_0, cannot be clearly defined since it involves, in unknown proportions, tissue blood-volume fraction, tissue tracer-transport-rate constants and, for a small part that is usually not identified, decay-corrected IF. Furthermore, the Y_0

outcome may be affected by substantial measurement uncertainty from a variety of origins. We therefore believe that the use of Y_0 as a relevant metrics should be seriously questioned. Furthermore, considering a composite PGA metrics as the ratio between slope and Y_0, whose meaning is even more unclear than that of Y_0 and whose measurement uncertainty is very likely greater than that of Y_0 alone, calls for caution [5, 14].

Compliance with ethical standards

Ethics approval and consent to participate This is a theoretical study.

Consent for publication Not applicable.

Competing interests The authors declare that they have no competing interests.

References

1. Boellaard R. Standards for PET image acquisition and quantitative data analysis. J Nucl Med. 2009;50:11S–20S.
2. Patlak CS, Blasberg RG, Fenstermacher JD. Graphical evaluation of blood-to brain transfer constants from multiple-time uptake data. J Cereb Blood Flow Metab. 1983;3:1–7.
3. Patlak CS, Blasberg RG. Graphical evaluation of blood-to-brain transfer constants from multiple-time uptake data: generalizations. J Cereb Blood Flow Metab. 1985;5:584–90.
4. Carson RE. Tracer kinetic modeling in PET. In: Bailey DL, Townsend DW, Valk PE, Maisey MN, editors. Positron emission tomography, basic science and clinical practice. London: Springer; 2003. p. 147–79.
5. Coello C, Fisk M, Mohan D, et al. Quantitative analysis of dynamic (18)F-FDG PET/CT for measurement of lung inflammation. EJNMMI Res. 2017;7:47–59.
6. Rahmim A, Lodge MA, Karakatsanis NA, et al. Dynamic whole-body PET imaging: principles, potentials and applications. Eur J Nucl Med Mol Imaging. 2019;46:501–18.
7. Zhang X, Xie Z, Berg E, et al. Total-body dynamic reconstruction and parametric imaging on the uEXPLORER. J Nucl Med. 2020;61:285–91.
8. Hunter GJ, Hamberg LM, Alpert NM, Choi NC, Fischman AJ. Simplified measurement of deoxyglucose utilization rate. J Nucl Med. 1996;37:950–5.
9. Van den Hoff J, Hofheinz F, Oehme L, et al. Dual time point based quantification of metabolic uptake rates in 18F-FDG PET. EJNMMI Res. 2013;3:16–27.
10. Vriens D, Disselhorst JA, Oyen WJG, de Geus-Oei L-F, Visser EP. Quantitative assessment of heterogeneity in tumor metabolism using FDG-PET. Int J Radiation Oncol Biol Phys. 2012;82:e725–31.
11. Laffon E, Marthan R. The total amount of uptake may affect the input function: a theoretic approach about 18F-FDG PET imaging. Nucl Med Biol. 2015;42:724–7.
12. Weber WA, Ziegler SI, Thödtmann R, Hanauske A-R, Schwaiger M. Reproducibility of metabolic measurements in malignant tumors using FDG PET. J Nucl Med. 1999;40:1771–7.
13. Laffon E, Calcagni ML, Galli G, Giordano A, Capotosti A, Marthan R, et al. Comparison of three-parameter kinetic model analysis to standard Patlak's analysis in ^{18}F-FDG PET imaging of lung cancer patients. EJNMMI Res. 2018;8:24–32.
14. JCGM 100: 2008. Evaluation of measurement data – Guide to the expression of uncertainty in measurement; 2008. Available at: http://www.bipm.org.